

1 Interaction of CO₂ concentrations and water stress in 2 semi-arid plants causes diverging response in instantaneous 3 water use efficiency and carbon isotope composition

4 Na Zhao^{1,3}, Ping Meng², Yabing He¹, Xinxiao Yu^{1,3*}

5 ¹ College of soil and water conservation, Beijing Forestry University, Beijing 100083, P.R. China

6 ² Research Institute of Forestry, Chinese Academy of Forestry 100091, Beijing, P.R. China

7 ³ Beijing collaborative innovation center for eco-environmental improvement with forestry and
8 fruit trees

9 **Abstract.** In the context of global warming attributable to the increasing levels of CO₂, severe drought
10 may be more frequent in areas with chronic water shortages (semi-arid areas). This necessitates
11 research on the interactions between increased levels of CO₂ and drought on plant photosynthesis. It is
12 commonly reported that ¹³C fractionation **occurs** as CO₂-gas diffuses from the atmosphere to the
13 sub-stomatal cavity. Few researchers have investigated ¹³C fractionation at the site of carboxylation to
14 cytoplasm before sugars are exported outward from the leaf. This process typically progresses in
15 response to variations in environmental conditions (i.e., CO₂ concentrations and water stress),
16 including in their interaction. Therefore, saplings of two typical plant species (*Platycladus orientalis*
17 and *Quercus variabilis*) from semi-arid areas of Northern China were selected and cultivated in growth
18 chambers with orthogonal treatments (four CO₂ concentrations ([CO₂]) × five soil volumetric water
19 contents (SWC)). The δ¹³C of water-soluble compounds extracted from leaves of saplings was
20 determined for instantaneous water use efficiency (WUE_{cp}) after cultivation. Instantaneous water use
21 efficiency derived from gas exchange (WUE_{ge}) was integrated to estimate differences in δ¹³C signal
22 variation before leaf-level translocation of primary assimilates. The WUE_{ge} of *P. orientalis* and *Q.*
23 *variabilis* both decreased with increased soil moisture at 35%–80% of field capacity (FC), and
24 increased with elevated [CO₂] by increasing photosynthetic capacity and reducing transpiration.
25 Instantaneous water use efficiency (iWUE) according to environmental changes, differed between the
26 two species. The WUE_{ge} in *P. orientalis* was significantly greater than that in *Q. variabilis*, while an
27 opposite trend was observed when comparing WUE_{cp} between the two species. Total ¹³C fractionation
28 at the site of carboxylation to cytoplasm before sugar export (total ¹³C fractionation) was
29 species-specific, as demonstrated in the interaction of [CO₂] and SWC. Rising [CO₂] coupled with
30 moistened soil generated increasing disparities in δ¹³C between water-soluble compounds (δ¹³C_{wsc})
31 and estimates based on gas-exchange observations (δ¹³C_{obs}) in *P. orientalis*, ranging between
32 0.0328‰–0.0472‰. Differences between δ¹³C_{wsc} and δ¹³C_{obs} in *Q. variabilis* increased as [CO₂] and
33 SWC increased (0.0384‰–0.0466‰). The ¹³C **fractionation** from mesophyll conductance (*g_m*) and
34 post-carboxylation both contributed to the total ¹³C fractionation that was determined by δ¹³C of
35 water-soluble compounds and gas-exchange **measurements**. Total ¹³C fractionation was linearly
36 dependent on stomatal conductance, indicating post-carboxylation fractionation could be attributed to
37 environmental variation. The magnitude and environmental dependence of apparent post-carboxylation
38 fractionation is worth our attention when addressing photosynthetic fractionation.

39 **Key words:** Post-carboxylation fractionation; Carbon isotope fractionation; Elevated CO₂
40 concentration; Soil volumetric water content; Instantaneous water use efficiency

41 **1 Introduction**

42 Since the industrial revolution, atmospheric CO₂ concentration has increased at an annual rate of
43 0.4%, and is expected to increase to 700 μmol·mol⁻¹, culminating in more frequent periods of dryness
44 (IPCC, 2014). Increasing atmospheric CO₂ concentrations that exacerbate the greenhouse effect will
45 increase fluctuations in global precipitation patterns, but will probably amplify drought frequency in
46 arid regions, and lead to more frequent extreme events in humid regions (Lobell et al., 2014).
47 Accompanying the increasing concentration of CO₂, mean δ¹³C of atmospheric CO₂ is currently being
48 depleted by 0.02‰–0.03‰ year⁻¹ (CU-INSTAAR/NOAACMDL network for atmospheric CO₂;
49 <http://www.esrl.noaa.gov/gmd/>).

50 The current carbon isotopic composition may respond to environmental change and their influence
51 on diffusion via plant physiological and metabolic processes (Gessler et al., 2014; Streit et al., 2013).
52 While depletion of δ¹³C_{CO₂} is occurring in the atmosphere, variations in CO₂ concentration ([CO₂])
53 may affect δ¹³C of plant organs that, in turn, are responding physiologically to changes in climate
54 (Gessler et al., 2014). The carbon discrimination (¹³Δ) of leaves could also provide timely feedback
55 about the availability of soil moisture and the atmospheric vapor pressure deficit (Cernusak et al.,
56 2012). Discrimination of ¹³C in leaves relies mainly on environmental factors that affect the ratio of
57 intercellular to ambient [CO₂] (*C_i/C_a*). Rubisco activities and the mesophyll conductance derived from
58 the difference of [CO₂]s between intercellular sites and chloroplasts are also involved (Farquhar et al.,
59 1982; Cano et al., 2014). Changes in environmental conditions affect photosynthetic discrimination,
60 recording differentially in the δ¹³C of water-soluble compounds (δ¹³C_{WSC}) in different plant organs.
61 Several processes during photosynthesis alter the δ¹³C of carbon transported within plants.
62 Carbon-fractionation during photosynthetic CO₂ fixation has been reviewed elsewhere (Farquhar et al.,
63 1982; Farquhar and Sharkey, 1982).

64 Post-photosynthetic fractionation is derived from equilibrium and kinetic isotopic effects that
65 determine isotopic differences between metabolites and intramolecular reaction positions. These are
66 defined as “post-photosynthetic” or “post-carboxylation” fractionation (Jäggi et al., 2002; Badeck et al.,
67 2005; Gessler et al., 2008). Post-carboxylation fractionation in plants includes the carbon
68 discrimination that follows carboxylation of ribulose-1, 5-bisphosphate, and internal diffusion (RuBP,
69 27‰), as well as related transitory starch metabolism (Gessler et al., 2008; Gessler et al., 2014)
70 fractionation in leaves, fractionation-associated phloem transport, remobilization or storage of soluble
71 carbohydrates, and starch metabolism fractionation in sink tissue (tree rings). In the synthesis of
72 soluble sugars, ¹³C-depletions of triose phosphates occur during export from the cytoplasm, and during
73 production of fructose-1, 6-bisphosphate by aldolase in transitory starch synthesis (Rossmann
74 et al., 1991; Gleixner and Schmidt, 1997). Synthesis of sugars before transportation to the twig is
75 associated with the post-carboxylation fractionation generated in leaves. Although these are likely to
76 play a role, another consideration is [CO₂] in the chloroplast (*C_c*), not in the intercellular space, as used
77 in the simplified equation of Farquhar’s model (Evans et al., 1986; Farquhar et al., 1989) is actually
78 defined as carbon isotope discrimination (δ¹³C). Differences between gas-exchange derived values and
79 online measurements of δ¹³C have often been used to estimate *C_i-C_c* and mesophyll conductance for
80 CO₂ (Le Roux et al., 2001; Warren and Adams, 2006; Flexas et al., 2006; Evans et al., 2009; Flexas et
81 al., 2012; Evans and von Caemmerer 2013). In this regard, changes in mesophyll conductance could be

82 partly responsible for the differences in two measurements, as it generally increases in the short term in
83 response to elevated CO₂ (Flexas et al., 2014), but it tends to decrease under drought (Hommel et al.,
84 2014; Théroux-Rancourt et al., 2014). Therefore, it is necessary to avoid confusion between carbon
85 isotope discrimination derived from synthesis of soluble sugars and/or mesophyll conductance. The
86 degree to which carbon fractionation is related to environmental variation has yet to be fully
87 investigated.

88 The simultaneous isotopic analysis of leaves allows determination of temporal variation in isotopic
89 fractionation (Rinne et al., 2016). This will aid in the accurate recording of environmental conditions.
90 Newly assimilated carbohydrates can be extracted, and these are termed the water-soluble compounds
91 (WSCs) in leaves (Brandes et al., 2006; Gessler et al., 2009). WSCs can also be associated with an
92 assimilation-weighted mean of C_i/C_a (and C_c/C_a) photosynthesized over periods ranging from a few
93 hours to 1–2 day (Pons et al., 2009). However, there is disagreement whether fractionation caused by
94 post-carboxylation and/or mesophyll resistance can alter the stable signatures of leaf carbon and thence
95 influence instantaneous water use efficiency (iWUE). In addition, the manner in which iWUE derived
96 from isotopic fractionation responds to environmental factors, such as elevated [CO₂] and/or soil water
97 gradients, is unknown.

98 Consequently, we investigated the $\delta^{13}\text{C}$ of fast-turnover carbohydrate pool in sapling leaves of two
99 tree species, *Platycladus orientalis* (L.) Franco and *Quercus variabilis* Bl., native to semi-arid areas of
100 China. We conducted gas-exchange measurements in controlled environment growth chambers
101 (FH-230, Taiwan Hipoint Corporation, Kaohsiung City, Taiwan). One goal is to differentiate the ¹³C
102 fractionation from the site of carboxylation to cytoplasm prior to sugar transportation in *P. orientalis*
103 and *Q. variabilis*, that is the total ¹³C fractionation, determined from the $\delta^{13}\text{C}$ of WSCs and
104 gas-exchange measurements. Another goal is to discuss the potential causes for the observed
105 divergence, estimate contributions of post-photosynthesis and mesophyll conductance on these
106 differences, and describe how carbon isotopic fractionation responds to the interactive effects of
107 elevated [CO₂] and water stress.

108 2 Material and Methods

109 2.1 Study site and design

110 *P. orientalis* and *Q. variabilis* saplings, selected as experimental material, were obtained from the
111 Capital Circle forest ecosystem station, a part of Chinese Forest Ecosystem Research Network
112 (CFERN), 40°03'45"N, 116°5'45"E in Beijing, China. This region is forested by *P. orientalis* and *Q.*
113 *variabilis*. We chose saplings of similar basal diameters, heights, and growth class. Each sapling was
114 placed into an individual pot (22 cm diam. × 22 cm high). Undisturbed soil samples were collected
115 from the field, sieved (with particles >10 mm removed), and placed into the pots. The soil bulk density
116 in the pots was maintained at 1.337–1.447 g cm⁻³. After a 30-day transplant recovery period, the
117 saplings were placed into growth chambers for orthogonal cultivation.

118 The controlled experiment was conducted in growth chambers (FH-230, Taiwan Hipoint
119 Corporation, Kaohsiung City, Taiwan). To reproduce the meteorological conditions of different
120 growing seasons in the research region, daytime and nighttime temperatures in the chambers were set
121 to 25 ± 0.5°C from 07:00 to 17:00 and 18 ± 0.5°C from 17:00 to 07:00. Relative humidity was
122 maintained at 60% and 80% during the daytime and nighttime, respectively. The mean daytime light
123 intensity was 200–240 μmol m⁻² s⁻¹. The chamber system can both control and monitor [CO₂]. Two

124 growth chambers (A and B) were used in this study. Chamber A maintained [CO₂]s at 400 ppm (C₄₀₀)
125 and 500 ppm (C₅₀₀). Chamber B maintained [CO₂]s at 600 ppm (C₆₀₀) and 800 ppm (C₈₀₀). The target
126 [CO₂] in each chamber had a standard deviation of ± 50 ppm during plant cultivation and testing.

127 An automatic watering device was used to irrigate the potted saplings to avoid heterogeneity when
128 scheduled watering was not made (Fig. 1). The watering device consisted of a water storage tank,
129 holder, controller, soil moisture sensors, and drip irrigation component. Prior to use, the tank was filled
130 with water, and the soil moisture sensor was inserted to a uniform depth in the soil. After connecting
131 the controller to an AC power supply, target soil volumetric water content (SWC) could be set and
132 monitored by soil moisture sensors. Since changes in SWC could be sensed by the sensors, this
133 automatic watering device can be regulated to begin watering or stop watering the plants. One
134 irrigation device was installed per chamber. Based on mean field capacity (FC) of potted soil (30.70%),
135 we established orthogonal treatments of four [CO₂]s × five SWCs (Tab. 1). In Table 1, A₁-A₄ denotes
136 [CO₂] of 400 ppm (C₄₀₀), 500 ppm (C₅₀₀), 600 ppm (C₆₀₀) and 800 ppm (C₈₀₀) in the chambers; B₁-B₅
137 denotes 35%–45% of FC (10.74%–13.81%), 50%–60% of FC (15.35%–18.42%), 60%–70% of FC
138 (18.42%–21.49%), and 70%–80% of FC (21.49%–24.56%) and 100% of FC (CK, 27.63%–30.70%).
139 Each orthogonal treatment of [CO₂] × SWC for two saplings per species was repeated twice. Each
140 treatment lasted 7 days. One pot was exposed in each of the [CO₂] × SWC treatments. Pots in the
141 chambers were rearranged every two days to promote uniform illumination.

142 2.2 Foliar gas exchange measurement

143 Fully expanded primary annual leaves of the saplings were measured with a portable infrared gas
144 photosynthesis system (LI-6400, Li-Cor, Lincoln, US) before and after the 7-day cultivation. Two
145 saplings per species were replicated per treatment (SWC × [CO₂]). For each sapling, four leaves were
146 sampled and four measurements were conducted on each leaf. Main photosynthetic parameters, such as
147 net photosynthetic rate (P_n) and transpiration rate (T_r), were measured. Based on theoretical
148 considerations of Von Caemmerer and Farquhar (1981), stomatal conductance (g_s) and intercellular
149 [CO₂] (C_i) were calculated by the Li-Cor software. Instantaneous water use efficiency via gas exchange
150 (WUE_{ge}) was calculated as the ratio P_n / T_r .

151 2.3 Plant material collection and leaf water-soluble compounds extraction

152 Eight recently-expanded sun leaves were selected per sapling and homogenized in liquid nitrogen
153 after gas-exchange measurements were finished. For extraction of WSCs from the leaves (Gessler et
154 al., 2004), 50 mg of ground leaves and 100 mg of PVPP (polyvinylpyrrolidone) were mixed and
155 incubated in 1 mL distilled water for 60 min at 5°C in a centrifuge tube. Each leaf sample was
156 replicated twice. Two saplings per species were chosen for each orthogonal treatment. The tubes
157 containing the mixture were heated in 100°C water for 3 min. After cooling to room temperature, the
158 supernatant of the mixture was centrifuged (12000 × g for 5 min) and 10 µL of supernatant was
159 transferred into a tin capsule and dried at 70°C. Folded capsules were used for δ¹³C analysis of WSCs.
160 The samples of WSCs from leaves were combusted in an elemental analyzer (EuroEA, HEKAtech
161 GmbH, Wegberg, Germany) and analyzed with a mass spectrometer (DELTA^{plus}XP, ThermoFinnigan).

162 Carbon isotope signatures were expressed in δ-notation (parts per thousand), relative to the
163 international Pee Dee Belemnite (PDB) standard:

$$164 \delta^{13}\text{C} = \left(\frac{R_{\text{sample}}}{R_{\text{standard}}} - 1 \right) \times 1000 \quad (1)$$

165 where δ¹³C is the heavy isotope and R_{sample} and R_{standard} refer to the isotope ratio between the particular

166 substance and the corresponding standard, respectively. The precision of repeated measurements was
167 0.1 ‰.

168 2.4 Isotopic calculation

169 2.4.1 ¹³C fractionation from the site of carboxylation to cytoplasm prior to **sugar** transportation

170 Based on the linear model of Farquhar and Sharkey (1982), the isotope discrimination, Δ , was
171 calculated as

$$172 \Delta = (\delta^{13}C_a - \delta^{13}C_{WSC}) / (1 + \delta^{13}C_{WSC}), \quad (2)$$

173 where $\delta^{13}C_a$ and $\delta^{13}C_{WSC}$ are the isotope signatures of ambient [CO₂] in chambers and WSCs extracted
174 from leaves, respectively. The $C_i:C_a$ was determined by

$$175 C_i:C_a = (\Delta - a) / (b - a), \quad (3)$$

176 where C_i and C_a are the [CO₂]s within substomatal cavities and in **growth** chambers, respectively; a is
177 the fractionation occurring CO₂ diffusion in still air (4‰) and b refers to the discrimination during CO₂
178 fixation by ribulose 1,5- biphosphate carboxylase/oxygenase (Rubisco) and internal diffusion (30‰).
179 Instantaneous water use efficiency by gas-exchange **measurement** (WUE_{ge}) was calculated as

$$180 WUE_{ge} = P_n:T_r = (C_a - C_i) / 1.6\Delta e, \quad (4)$$

181 where 1.6 is the diffusion ratio of stomatal conductance for water vapor to CO₂ in chambers and Δe is
182 the difference between e_{lf} and e_{atm} , **representing** the extra- and intra-cellular water vapor pressure,
183 respectively:

$$184 \Delta e = e_{lf} - e_{atm} = 0.611 \times e^{17.502T/(240.97+T)} \times (1 - RH), \quad (5)$$

185 where T and RH are the temperature and relative humidity on leaf surface, respectively. Combining
186 Eqns. (2, 3 and 4), the instantaneous water use efficiency could be determined by the $\delta^{13}C_{WSC}$ of leaves,
187 defined as:

$$188 WUE_{cp} = \frac{P_n}{T_r} = (1 - \varphi) (C_a - C_i) / 1.6\Delta e = C_a(1 - \varphi) \left[\frac{b - \delta^{13}C_a + (b+1)\delta^{13}C_{WSC}}{(b-a)(1 + \delta^{13}C_{WSC})} \right] / 1.6\Delta e, \quad (6)$$

189 where φ is the respiratory ratio of leaf carbohydrates to other organs at night (0.3).

190 Then the ¹³C fractionation from the site of carboxylation to cytoplasm prior to sugars transportation
191 (defined as the total ¹³C fractionation) was estimated by the observed $\delta^{13}C$ of WSCs from leaves
192 ($\delta^{13}C_{WSC}$) and the modeled $\delta^{13}C$ calculated from gas-exchange measurements ($\delta^{13}C_{model}$). The $\delta^{13}C_{model}$
193 was calculated from Δ_{model} from Eqn. (2); Δ_{model} was determined by **combining** Eqns. (3 and 4) as

$$194 \Delta_{model} = (b - a) \left(1 - \frac{1.6\Delta e WUE_{ge}}{C_a} \right) + a, \quad (7)$$

$$195 \delta^{13}C_{model} = \frac{C_a - \Delta_{model}}{1 + \Delta_{model}}, \quad (8)$$

$$196 \text{Total } ^{13}\text{C fractionation} = \delta^{13}C_{WSC} - \delta^{13}C_{model}. \quad (9)$$

197 2.4.2 Method of estimations for mesophyll conductance and the contribution of post-carboxylation
198 fractionation

199 The carbon isotope discrimination was generated from the relative contribution of diffusion and
200 carboxylation, reflected by the ratio of [CO₂] at the site of carboxylation (C_c) to the **concentration** in the

201 **outside air** (C_a). The carbon isotopic discrimination (Δ) can be presented as (Farquhar et al. 1982):

$$202 \quad \Delta = a_b \frac{C_a - C_s}{C_a} + a \frac{C_s - C_i}{C_a} + (e_s + a_l) \frac{C_i - C_c}{C_a} + b \frac{C_c}{C_a} - \frac{eR_D + f\Gamma^*}{C_a}, \quad (10)$$

203 where C_a , C_s , C_i , and C_c are the $[\text{CO}_2]$ s in the ambient **air**, at the boundary layer of the leaf, in the
 204 substomatal cavities, and at the sites of carboxylation, respectively; a_b is the CO_2 diffusional
 205 fractionation at the boundary layer (2.9‰); e_s is the discrimination for CO_2 diffusion when CO_2 enters
 206 in solution (1.1‰, at 25°C); a_l is the CO_2 diffusional fractionation in the liquid phase (0.7‰); e and f
 207 are carbon discriminations derived in dark respiration (R_D) and photorespiration, respectively; k is the
 208 carboxylation efficiency, and Γ^* is the CO_2 compensation point in the absence of dark respiration
 209 (Brooks and Farquhar, 1985).

210 When gas in the cuvette is well stirred during gas-exchange measurements, diffusion **across the**
 211 boundary layer could be neglected and **Eqn. (10)** can be **written** as

$$212 \quad \Delta = a \frac{C_a - C_i}{C_a} + (e_s + a_l) \frac{C_i - C_c}{C_a} + b \frac{C_c}{C_a} - \frac{eR_D + f\Gamma^*}{C_a}. \quad (11)$$

213 There is no consensus about the value of e , although recent measurements estimate it as ranging
 214 from 0-4‰. The value of f has been estimated to range from 8-12‰ (Gillon and Griffiths, 1997;
 215 Igamberdiev et al., 2004; Lanigan et al., 2008). As the most direct factor, b **influences** the calculation of
 216 g_m , which is thought to be approximately 30‰ in higher plants (Guy et al., 1993).

217 The difference of $[\text{CO}_2]$ between substomatal cavities and chloroplasts is **omitted**, while **diffusion**
 218 related to dark-respiration and photorespiration are negligible and **Eqn. (11)** may be simplified to

$$219 \quad \Delta_i = a + (b - a) \frac{C_i}{C_a}. \quad (12)$$

220 **Eqn. (12)** denotes the linear relationship between carbon discrimination and C_i/C_a . That underlines
 221 subsequent comparison between expected Δ (originating from gas-exchange, Δ_i , and actually measured
 222 Δ_{obs}), could evaluate the differences of $[\text{CO}_2]$ between intercellular air and sites of carboxylation that
 223 are the ^{13}C fractionation from mesophyll conductance. Consequently, g_m is calculated by subtracting the
 224 Δ_{obs} of **Eqn. (11)** from Δ_i (**Eqn. (12)**):

$$225 \quad \Delta_i - \Delta_{obs} = (b - e_s - a_l) \frac{C_i - C_c}{C_a} + \frac{eR_D + f\Gamma^*}{C_a} \quad (13)$$

226 and P_n from Fick's first law is presented by

$$227 \quad P_n = g_m(C_i - C_c). \quad (14)$$

228 Substituting **Eqn. (14)** into **Eqn. (13)** we obtain

$$229 \quad \Delta_i - \Delta_{obs} = (b - e_s - a_l) \frac{P_n}{g_m C_a} + \frac{eR_D + f\Gamma^*}{C_a}, \quad (15)$$

$$230 \quad g_m = \frac{(b - e_s - a_l) \frac{P_n}{C_a}}{(\Delta_i - \Delta_{obs}) - \frac{eR_D + f\Gamma^*}{C_a}}. \quad (16)$$

231 In **the** calculation of g_m , terms of respiratory and photorespiratory could be ignored and e and f are
 232 assumed to be zero or to be cancelled out in the calculation of g_m .

233 Then **Eqn. (16)** can be **rewritten** as

$$g_m = \frac{(b-e_s-a_i) \frac{P_n}{C_a}}{\Delta_i - \Delta_{obs}} \quad (17)$$

Therefore, the contribution of post- carboxylation fractionation can be estimated by

$$\text{Contribution of post - carboxylation fractionation} = \frac{(\text{Total } ^{13}\text{C fractionation} - \text{fractionation from mesophyll conductance})}{\text{Total } ^{13}\text{C fractionation}} \times 100\% \quad (18)$$

3 Results

3.1 Foliar gas exchange measurements

When SWC increased between the treatments, P_n , g_s and T_r in *P. orientalis* and *Q. variabilis* peaked at 70%–80% of FC and/or 100% of FC (Fig. 2). The C_i in *P. orientalis* rose as SWC increased. It peaked at 60%–70% of FC and declined thereafter with increased SWC in *Q. variabilis*. The carbon uptake and C_i were significantly improved by elevated $[\text{CO}_2]$ at all SWCs for the two species ($p < 0.05$). Greater increases of P_n in *P. orientalis* were found at 50%–70% of FC from C_{400} to C_{800} , which was at 35%–45% of FC in *Q. variabilis*. As water stress was reduced (at 70%–80% of FC and 100% of FC), reduction of g_s in *P. orientalis* was more pronounced with elevated $[\text{CO}_2]$ at a given SWC ($p < 0.01$). Nevertheless, g_s in *Q. variabilis* for C_{400} , C_{500} , and C_{600} was significantly higher than for C_{800} at 50%–80% of FC ($p < 0.01$). Coordinated with g_s , T_r of the two species for C_{400} and C_{500} was significantly higher than for C_{600} and C_{800} , except at 35%–60% of FC ($p < 0.01$, Figs. 2g and 2h). P_n , g_s , C_i and T_r in *Q. variabilis* was significantly greater than the corresponding values in *P. orientalis* ($p < 0.01$, Fig. 2).

3.2 $\delta^{13}\text{C}$ of water-soluble compounds in leaves

After observations of photosynthetic traits in leaves of the two species, the same leaves were immediately frozen and WSCs were extracted for all orthogonal treatments. The carbon isotope composition of WSCs ($\delta^{13}\text{C}_{\text{WSC}}$) of both species increased as SWC increased (Figs. 3a and 3b, $p < 0.01$). The mean $\delta^{13}\text{C}_{\text{WSC}}$ of *P. orientalis* and *Q. variabilis* ranged from $-27.44 \pm 0.155\%$ to $-26.71 \pm 0.133\%$, and from $-27.96 \pm 0.129\%$ to $-26.49 \pm 0.236\%$, respectively. The photosynthetic capacity varied with increased SWC and the mean $\delta^{13}\text{C}_{\text{WSC}}$ of the two species, reaching their respective maxima at 70%–80% of FC. With gradual enrichment of $[\text{CO}_2]$, mean $\delta^{13}\text{C}_{\text{WSC}}$ in both species declined when $[\text{CO}_2]$ exceeded 600 ppm ($p < 0.01$). Except for C_{400} at 50%–100% of FC, the $\delta^{13}\text{C}_{\text{WSC}}$ in *P. orientalis* was significantly larger than that in *Q. variabilis* at any $[\text{CO}_2] \times \text{SWC}$ treatment ($p < 0.01$, Fig. 3).

3.3 Estimations of WUE_{ge} and WUE_{cp}

Figure 4a shows that increments of WUE_{ge} in *P. orientalis* under severe drought (i.e., 35%–45% of FC) were highest at any $[\text{CO}_2]$, ranging from 90.70% to 564.65%. The WUE_{ge} in *P. orientalis* decreased as SWC increased, while values increased as $[\text{CO}_2]$ increased. Differing from variation in WUE_{ge} in *P. orientalis* with moistened soil, WUE_{ge} in *Q. variabilis* increased slightly at 100% of FC for C_{600} or C_{800} (Fig. 4b). The maximum WUE_{ge} occurred at 35%–45% of FC for C_{800} among all orthogonal treatments associated with both species. Elevated $[\text{CO}_2]$ enhanced the WUE_{ge} in *Q. variabilis* at any SWC, except at 60%–80% of FC. Thirty-two saplings of *P. orientalis* had greater WUE_{ge} than did *Q. variabilis* for the same $[\text{CO}_2] \times \text{SWC}$ treatments ($p < 0.05$).

As illustrated in Fig. 5a, WUE_{cp} in *P. orientalis* for C_{600} or C_{800} increased as water stress was alleviated beyond 50%–60% of FC, as well as that for C_{400} or C_{500} , while SWC exceeded 60%–70% of FC. *Q. variabilis* showed variable WUE_{cp} with increasing SWC (Fig. 5b). Except for C_{400} , WUE_{cp} in *Q.*

273 *variabilis* decreased abruptly at 50%–60% of FC, and then increased as SWC increased for C₅₀₀, C₆₀₀,
274 and C₈₀₀. In contrast to the results for WUE_{ge}, WUE_{cp} in *Q. variabilis* was more pronounced than in *P.*
275 *orientalis* among all orthogonal treatments.

276 3.4 ¹³C fractionation from the site of carboxylation to cytoplasm before sugar transportation

277 We evaluated the total ¹³C fractionation from the site of carboxylation to the cytoplasm by
278 gas-exchange measurements and WSCs in leaves (Table 2), which can help track the path of ¹³C
279 fractionation in leaves. Comparing δ¹³C_{WSC} with δ¹³C_{model} from Eqns. (4, 7–9), the total ¹³C
280 fractionation in *P. orientalis* ranged from 0.0328‰ to 0.0472‰, which was less than that in *Q.*
281 *variabilis* (0.0384‰ to 0.0466‰). The total fractionation in *P. orientalis* was magnified with
282 increasing SWC especially when SWC reached 35%–80% of FC from C₄₀₀ to C₈₀₀ (increased by
283 21.30%–42.04%). The total fractionation for C₄₀₀ and C₅₀₀ were amplified as SWC increased until
284 50%–60% of FC in *Q. variabilis*, whereas they were increased at 50%–80% of FC and decreased at
285 100% of FC for C₆₀₀ and C₈₀₀. Elevated [CO₂] enhanced the mean total fractionation in *P. orientalis*,
286 while fractionation in *Q. variabilis* declined sharply from C₆₀₀ to C₈₀₀. Total ¹³C fractionation, with
287 increased SWC, in *P. orientalis* increased more rapidly than it did in *Q. variabilis*.

288 3.5 g_m imposed on the interaction of CO₂ concentration and water stress

289 A comparison between online leaf δ¹³C_{WSC} and the values of gas-exchange measurements is given to
290 estimate the g_m over all treatments in Fig. 6 (Eqns. (10–17)). A significant increasing trend occurred in
291 g_m with decreasing water stress in *P. orientalis*, ranging from 0.0091–0.0690 mol CO₂ m⁻² s⁻¹ (p < 0.05),
292 which reached a maximum at 100% of FC under a given [CO₂]. Increases in g_m in *Q. variabilis* with
293 increasing SWC were not significant, except those under C₄₀₀. With increasing [CO₂], g_m in the two
294 species increased at different rates. With *P. orientalis* under C₄₀₀, g_m increased gradually and reached a
295 maximum under C₈₀₀ at 35%–60% of FC and 100% of FC (p < 0.05). However, that was maximized
296 under C₆₀₀ (p < 0.05) and reduced under C₈₀₀ at 60%–80% of FC. The maximum increment in g_m
297 (8.2%–58.4%) occurred at C₈₀₀ at all SWCs in *Q. variabilis*. The g_m in *Q. variabilis* was clearly greater
298 than that in *P. orientalis* under the same treatments.

299 3.6 Contribution of post-carboxylation fractionation

300 We evaluated the difference between Δ_i and Δ_{obs} in ¹³C fractionation derived from mesophyll
301 conductance. The post-photosynthetic fractionation after carboxylation can be calculated by subtracting
302 g_m-sourced fractionation from the total ¹³C fractionation (Table 2). The g_m-sourced fractionation
303 provided a smaller contribution to the total ¹³C fractionation than did post-carboxylation fractionation
304 irrespective of treatment (Table 2). The g_m-sourced fractionation in the two species illustrated different
305 variations with increasing SWC, which declined at 50%–80% of FC and increased at 100% of FC in *P.*
306 *orientalis*; yet, in *Q. variabilis*, it increased with water stress alleviation at 50%–80% of FC and then
307 decreased at 100% of FC. Nevertheless, in the two species post-carboxylation fractionation in leaves all
308 increased as SWC increased. The g_m-sourced fractionation in *P. orientalis* and *Q. variabilis* reached
309 their peaks under C₆₀₀ and C₈₀₀, respectively. Post-carboxylation fractionation was magnified with
310 [CO₂] increases in *P. orientalis*, and reached a maximum under C₆₀₀ and then declined under C₈₀₀.

311 3.7 Relationship between g_s, g_m and total ¹³C fractionation

312 Total ¹³C fractionation may be correlated with resistances associated with stomata and mesophyll
313 cells. We performed linear regressions between g_s/g_m and total ¹³C fractionation in *P. orientalis* and *Q.*
314 *variabilis* (Fig. 7 and 8). The total ¹³C fractionation was correlated to g_s (p < 0.01). The positive linear

315 relationships between g_m and total ^{13}C fractionation ($p < 0.01$) indicated that the variation of $[\text{CO}_2]$
316 through the chloroplast was correlated with carbon discrimination following leaf photosynthesis.

317 4 Discussion

318 4.1 Photosynthetic traits

319 The exchange of CO_2 and water vapor via stomata can be modulated by the soil/leaf water potential
320 (Robredo et al., 2010). Saplings of *P. orientalis* reached maximum P_n and g_s at 70%–80% of FC
321 irrespective of $[\text{CO}_2]$ treatments. As SWC exceeded this water threshold, elevated CO_2 caused a greater
322 reduction in g_s as is previously reported for barley and wheat (Wall et al., 2011). The decrease in g_s
323 responding to elevated $[\text{CO}_2]$, could be mitigated by increased SWC. The C_i in *Q. variabilis* peaked at
324 60%–70% of FC and then declined as soil moisture increased (Wall et al., 2006; Wall et al., 2011).
325 This may be because stomata tend to maintain a constant C_i or C_i/C_a when ambient $[\text{CO}_2]$ is increased,
326 which would determine the amount of CO_2 used directly in the chloroplast (Yu et al., 2010). This result
327 could be explained as stomatal limitation (Farquhar and Sharkey, 1982; Xu, 1997). However, C_i in *P.*
328 *orientalis* increased considerably, while SWC exceeded 70%–80% of FC, as found by Mielke et al.
329 (2000). One possible contributing factor is plants close their stomata to reduce water loss during
330 organic matter synthesis simultaneously decreasing the availability of CO_2 and generating respiration
331 of organic matter (Robredo et al., 2007). Another possible explanation is that the limited root volume of
332 potted plants may be unable to absorb sufficient water to support full growth of shoots (Leakey et al.,
333 2009; Wall et al., 2011). In the present study, increasing $[\text{CO}_2]$ may cause nonstomatal limitation when
334 SWC exceeds a soil moisture threshold of 70%–80% of FC. The accumulation of nonstructural
335 carbohydrates in leaf tissue may induce mesophyll-based and/or biochemical-based transient inhibition
336 of photosynthetic capacity (Farquhar and Sharkey, 1982). Xu and Zhou (2011) developed a five-level
337 SWC gradient to examine the effect of water on the physiology of perennial *Leymus chinensis* and
338 demonstrated that there was a clear maximum in SWC, below which the plant could adjust to changing
339 environmental conditions. Miranda Apodaca et al. (2015) also concluded that, in suitable water
340 conditions, elevated CO_2 levels augmented CO_2 assimilation in herbaceous plants.

341 The P_n of the two woody plant species increased with elevated $[\text{CO}_2]$ similar to results from other C_3
342 woody plants (Kgope et al., 2010). Increasing $[\text{CO}_2]$ alleviated severe drought and the need for heavy
343 irrigation, suggesting that photosynthetic inhibition produced by a lack or excess of water may be
344 mediated by increased $[\text{CO}_2]$ (Robredo et al., 2007; Robredo et al., 2010) and ameliorate the effects of
345 drought stress by reducing plant transpiration (Kirkham, 2016; Kadam et al., 2014; Miranda Apodaca
346 et al., 2015; Tausz Posch et al., 2013).

347 4.2 Differences between WUE_{ge} and WUE_{cp}

348 The increases in WUE_{ge} in *P. orientalis* and *Q. variabilis* that resulted from the combination of P_n
349 increase and g_s decrease were followed by a reduction in T_r (Figs. 2a, 2g, 2b and 2h). This result was
350 also demonstrated by Ainsworth and McGrath (2010). Comparing P_n and T_r in the two species, a lower
351 WUE_{ge} in *Q. variabilis* was obtained due to its physiological and morphological traits, such as larger
352 leaf area, rapid growth, and higher stomatal conductance than that in *P. orientalis* (Adiredjo et al.,
353 2014). Medlyn et al. (2001) reported that stomatal conductance of broadleaved species is more
354 sensitive to elevated $[\text{CO}_2]$ than conifer species. There is no agreement on the patterns of $i\text{WUE}$, at the
355 leaf level, related to SWC (Yang et al., 2010). The WUE_{ge} in *P. orientalis* and *Q. variabilis* were
356 enhanced with soil drying, as presented by Parker and Pallardy (1991), DeLucia and Heckathorn

357 (1989), Reich et al. (1989), and Leakey (2009).

358 Böggelein et al. (2012) confirmed that WUE_{cp} was more consistent with daily mean WUE_{ge} than
359 with WUE_{phloem} (calculated by the $\delta^{13}C$ of phloem). The WUE_{cp} of the two species demonstrated
360 similar variations to those in $\delta^{13}C_{WSC}$, which differed from those of WUE_{ge} . Pons et al. (2009) noted
361 that A of leaf soluble sugar is coupled with environmental dynamics over a period ranging from a few
362 hours to 1–2 days. The WUE_{cp} of our materials could respond to $[CO_2] \times SWC$ treatments over a
363 number of cultivated days, whereas WUE_{ge} is characterized as the instantaneous physiological change
364 in plants to new conditions. Consequently, WUE_{cp} and WUE_{ge} have different degrees of variations in
365 response to different treatments.

366 4.3 Influence of mesophyll conductance on the fractionation after carboxylation

367 CO_2 diffusion into photosynthetic sites includes two main processes. CO_2 first moves from ambient
368 air surrounding the leaf (C_a) through stomata to the sub-stomatic cavities (C_i). From sub-stomatic
369 cavities CO_2 then moves to the sites of carboxylation within the chloroplast stroma (C_c) of the leaf
370 mesophyll. The latter procedure of diffusion is termed mesophyll conductance (g_m ; Flexas et al., 2008).
371 Moreover, g_m has been identified to coordinate with environmental factors more rapidly than stomatal
372 conductance (Galmés et al., 2007; Tazoe et al., 2011; Flexas et al., 2007). During our 7-day cultivations
373 of $SWC \times [CO_2]$, g_m increased and WUE_{ge} decreased with increasing SWC. It has been documented
374 that g_m can improve WUE under drought pretreatment (Han et al., 2016). However, the mechanism in
375 which g_m responds to the fluctuation of $[CO_2]$ is unclear. Terashima et al. (2006) demonstrated that
376 CO_2 permeable aquaporin, located in the plasma membrane and inner envelope of chloroplasts, could
377 regulate the change in g_m . In our study, g_m is species-specific to the $[CO_2]$ gradient. The g_m in *P.*
378 *orientalis* significantly decreased by 9.08%-44.42% from C_{600} to C_{800} at 60%-80% of FC; these are
379 similar to the results of Flexas et al. (2007). A larger g_m in *Q. variabilis* under C_{800} was observed
380 compared with *P. orientalis*.

381 Furthermore, g_m contributed to the total ^{13}C fractionation that followed carboxylation, while
382 photosynthate had not been transported to the sapling twigs. The ^{13}C fractionation of CO_2 from the air
383 surrounding the leaf to sub-stomatic cavities may be simply explained by stomatal resistance, which
384 also contains the fractionation derived from mesophyll conductance between sub-stomatic cavities and
385 the site of carboxylation in the chloroplast that cannot be neglected and should be lucubrated (Pons et
386 al., 2009; Cano et al., 2014). In estimating the post-carboxylation fractionation, g_m -sourced
387 fractionation must be subtracted from the total ^{13}C fractionation (the difference between $\delta^{13}C_{WSC}$ and
388 $\delta^{13}C_{model}$), which is closely associated with g_m (Fig. 8, $p=0.01$). Variations in g_m -sourced fractionation
389 are coordinated with those in g_m with changing environmental conditions (Table 2).

390 4.4 Post-carboxylation fractionation generated before photosynthate moves out of leaves

391 Photosynthesis, a biochemical and physiological process (Badeck et al., 2005), is characterized by
392 discrimination in ^{13}C , which leaves an isotopic signature in the photosynthetic apparatus. Farquhar et al.
393 (1989) reviewed the carbon-fractionation in leaves and covered the significant aspects of
394 photosynthetic carbon isotope discrimination. The post-carboxylation/photosynthetic fractionation
395 associated with the metabolic pathways of non-structural carbohydrates (NSC; defined here as soluble
396 sugars + starch) within leaves, and fractionation during translocation, storage, and remobilization prior
397 to tree ring formation is unclear (Epron et al., 2012; Gessler et al., 2014; Rinne et al., 2016). The
398 synthesis of sucrose and starch before transportation to twigs falls within the domain of
399 post-carboxylation fractionation generated in leaves. Hence, we hypothesized that ^{13}C fractionation

400 might exist. When we completed the leaf gas-exchange measurements, leaf samples were collected
401 immediately to determine the $\delta^{13}\text{C}_{\text{WSC}}$. Presumably, ^{13}C fractionation generated in the synthetic
402 processes of sucrose and starch was contained within the ^{13}C fractionation from the site of
403 carboxylation to cytoplasm before **sugar** transportation. Comparing $\delta^{13}\text{C}_{\text{WSC}}$ with $\delta^{13}\text{C}_{\text{obs}}$, the total ^{13}C
404 fractionation **in** *P. orientalis* ranged from 0.0328‰ to 0.0472‰, which was somewhat less than that **in**
405 *Q. variabilis* (from 0.0384‰ to 0.0466‰). Post-carboxylation fractionation contributed 75.30%–98.9%
406 to total ^{13}C fractionation, determined by subtracting the fractionation **in** g_m from total ^{13}C fractionation.
407 Gessler et al. (2004) reviewed the environmental components of variation in photosynthetic carbon
408 isotope discrimination in terrestrial plants. Total ^{13}C fractionation **in** *P. orientalis* was enhanced by the
409 increase **in** SWC, consistent with that **in** *Q. variabilis*, except at 100% of FC. The ^{13}C isotope signature
410 **in** *P. orientalis* was depleted with elevated $[\text{CO}_2]$. Yet, ^{13}C -depletion was weakened in *Q. variabilis* **for**
411 C_{600} and C_{800} . Linear regressions between g_s and total ^{13}C fractionation indicated that the
412 post-carboxylation fractionation in leaves depends on the variation of g_s and **that stomata** aperture was
413 correlated with environmental change.

414 **5 Conclusions**

415 Through orthogonal treatments of four $[\text{CO}_2]_s \times$ five SWCs, WUE_{cp} calculated by $\delta^{13}\text{C}_{\text{WSC}}$ and
416 WUE_{ge} derived from simultaneous leaf gas-exchange, were estimated to differentiate the $\delta^{13}\text{C}$ signal
417 variation before leaf-level translocation of primary assimilates. The influence of g_m on ^{13}C fractionation
418 between the sites of carboxylation and **ambient air** is important. It requires consideration when testing
419 the hypothesis that the post-carboxylation contributes to the ^{13}C fractionation from the site of
420 carboxylation to cytoplasm before **sugar** transport. In response to the interactive effects of $[\text{CO}_2]$ and
421 SWC, WUE_{ge} **in the** two tree species both decreased with increasing SWC, and increased with elevated
422 $[\text{CO}_2]$ at 35%–80% of FC. We concluded that relative soil drying, coupled with elevated $[\text{CO}_2]$, can
423 improve WUE_{ge} by strengthening photosynthetic capacity and reducing transpiration. WUE_{ge} **in** *P.*
424 *orientalis* was significantly greater than that **in** *Q. variabilis*, while the opposite was the case for
425 WUE_{cp} . The g_m and post-carboxylation both contributed to the total ^{13}C fractionation. **Rising** $[\text{CO}_2]$
426 and/or moistening soil generated increasing disparities between $\delta^{13}\text{C}_{\text{WSC}}$ and $\delta^{13}\text{C}_{\text{model}}$ in *P. orientalis*;
427 nevertheless, the differences between $\delta^{13}\text{C}_{\text{WSC}}$ and $\delta^{13}\text{C}_{\text{model}}$ in *Q. variabilis* increased when $[\text{CO}_2]$ was
428 less than 600 ppm and/or water stress was alleviated. Total ^{13}C fractionation **in the** leaf was linearly
429 dependent on g_s . With respect to carbon isotope fractionation in post-carboxylation and transportation
430 processes, we note that ^{13}C fractionation derived from the synthesis of sucrose and starch is likely
431 influenced by environmental changes. A clear description of the magnitude and environmental
432 dependence of post-carboxylation fractionation is worth **considering**.

433 **References**

- 434 Adiredjo, A. L., Navaud, O., Lamaze, T., and Grieu, P.: Leaf carbon isotope discrimination as an
435 accurate indicator of water use efficiency in sunflower genotypes subjected to five stable soil
436 water contents, *J Agron. Crop Sci.*, 200, 416–424, 2014.
- 437 Ainsworth, E. A. and McGrath, J. M.: Direct effects of rising atmospheric carbon dioxide and ozone on
438 crop yields, *Climate Change and Food Security*, Springer, 109–130, 2010.
- 439 Badeck, F. W., Tcherkez, G., Eacute, N. S. S., Piel, C. E. M., and Ghashghaie, J.: Post-photosynthetic
440 fractionation of stable carbon isotopes between plant organ – a widespread phenomenon, *Rapid*

441 Commun. Mass S., 19, 1381–1391, 2005.

442 B ögelein, R., Hassdenteufel, M., Thomas, F. M., and Werner, W.: Comparison of leaf gas exchange
443 and stable isotope signature of water-soluble compounds along canopy gradients of co-occurring
444 Douglas-fir and European beech, *Plant Cell Environ.*, 35, 1245–1257, 2012.

445 Brandes, E., Kodama, N., Whittaker, K., Weston, C., Rennenberg, H., Keitel, C., Adams, M. A., and
446 Gessler, A.: Short-term variation in the isotopic composition of organic matter allocated from the
447 leaves to the stem of *Pinus sylvestris*: effects of photosynthetic and postphotosynthetic carbon
448 isotope fractionation, *Global Change Biol.*, 12, 1922–1939, 2006.

449 Brooks, A. and Farquhar, G. D.: Effect of temperature on the CO₂/O₂ specificity of
450 ribulose-1,5-bisphosphate carboxylase/oxygenase and the rate of respiration in the light, *Planta*,
451 165, 397–406, 1985.

452 Brugnoli E, Farquhar GD. 2000. Photosynthetic fractionation of carbon isotopes. In: Leegood RC,
453 Sharkey TD, von Caemmerer S. eds. Photosynthesis: physiology and metabolism. Advances in
454 photosynthesis. Dordrecht, The Netherlands: Kluwer Academic Publishers, 399–434.

455 Cano, F. J., López, R., and Warren, C. R.: Implications of the mesophyll conductance to CO₂ for
456 photosynthesis and water-use efficiency during long-term water stress and recovery in two
457 contrasting Eucalyptus species, *Plant Cell Environ.*, 37, 2470–2490, 2014.

458 Cernusak, L. A., Ubierna, N., Winter, K., Holtum, J. A. M., Marshall, J. D., and Farquhar, G. D.:
459 Environmental and physiological determinants of carbon isotope discrimination in terrestrial
460 plants, *New Phytologist*, 200, 950–965, 2013.

461 DeLucia, E. H. and Heckathorn, S. A.: The effect of soil drought on water-use efficiency in a
462 contrasting Great Basin desert and Sierran montane species, *Plant Cell Environ.*, 12, 935–940,
463 1989.

464 Epron, D., Nouvellon, Y., and Ryan, M. G.: Introduction to the invited issue on carbon allocation of
465 trees and forests, *Tree physiol.*, 32, 639–643, 2012.

466 Evans, J. R., Kaldenhoff, R., Genty, B., and Terashima, I.: Resistances along the CO₂ diffusion
467 pathway inside leaves, *J. Exp. Bot.*, 60, 2235–2248, 2009.

468 Evans, J. R., Sharkey, T. D., Berry, J. A., and Farquhar, G. D.: Carbon isotope discrimination measured
469 concurrently with gas-exchange to investigate CO₂ diffusion in leaves of higher-plants, *Funct.*
470 *Plant Biol.*, 13, 281–292, 1986.

471 Evans, J. R. and von Caemmerer, S.: Temperature response of carbon isotope discrimination and
472 mesophyll conductance in tobacco, *Plant Cell Environ.*, 36, 745–756, 2013.

473 Farquhar, G. D., Ehleringer, J. R., and Hubick, K. T.: Carbon isotope discrimination and
474 photosynthesis, *Ann. Rev. Plant Physiol.*, 40, 503–537, 1989.

475 Farquhar, G. D., O'Leary, M. H., and Berry, J. A.: On the relationship between carbon isotope
476 discrimination and the intercellular carbon dioxide concentration in leaves, *Funct. Plant Biol.*, 9,
477 121–137, 1982.

478 Farquhar, G. D. and Sharkey, T. D.: Stomatal conductance and photosynthesis, *Ann. Rev. Plant*
479 *Physiol.*, 33, 317–345, 1982.

480 Flexas, J., Barbour, M. M., Brendel, O., Cabrera, H. M., Carriqui í M., D áz-Espejo, A., Douthe, C.,
481 Dreyer, E., Ferrio, J. P., Gago, J., Gall é A., Galm és, J., Kodama, N., Medrano, H., Niinemets, Ü.,
482 Peguero-Pina, J. J., Pou, A., Ribas-Carbó M., Tomás, M., Tosens, T., and Warren, C. R.:
483 Mesophyll diffusion conductance to CO₂: An unappreciated central player in photosynthesis, *Plant*
484 *Science*, 193–194, 70–84, 2012.

485 Flexas, J., Carriquí M., Coopman, R. E., Gago, J., Galmés, J., Martorell, S., Morales, F., and
486 Diaz-Espejo, A.: Stomatal and mesophyll conductances to CO₂ in different plant groups:
487 Underrated factors for predicting leaf photosynthesis responses to climate change? *Plant Science*,
488 226, 41–48, 2014.

489 Flexas, J., Diaz-Espejo, A., Galmés, J., Kaldenhoff, R., Medano, H., and Ribas-Carbo, M.: Rapid
490 variations of mesophyll conductance in response to changes in CO₂ concentration around leaves,
491 *Plant Cell Environ.*, 30, 1284–1298, 2007.

492 Flexas, J., Ribas-Carbó M., Diaz-Espejo, A., Galmés, J., and Medrano, H.: Mesophyll conductance to
493 CO₂: current knowledge and future prospects, *Plant Cell Environ.*, 31, 602–621, 2008.

494 Flexas, J., Ribas-Carbó M., Hanson, D.T., Bota, J., Otto, B., Cifre, J., McDowell, N., Medrano, H., and
495 Kaldenhoff, R.: Tobacco aquaporin NtAQP1 is involved in mesophyll conductance to CO₂ *in vivo*,
496 *Plant J.*, 48, 427–439, 2006.

497 Galmés, J., Medrano, H., and Flexas, J.: Photosynthetic limitations in response to water stress and
498 recovery in Mediterranean plants with different growth forms, *New Phytol.*, 175, 81–93, 2007.

499 Gessler, A., Brandes, E., Buchmann, N., Helle, G., Rennenberg, H., and Barnard, R. L.: Tracing carbon
500 and oxygen isotope signals from newly assimilated sugars in the leaves to the tree-ring archive,
501 *Plant Cell Environ.*, 32, 780–795, 2009.

502 Gessler, A., Ferrio, J. P., Hommel, R., Treydte, K., Werner, R. A., and Monson, R. K.: Stable isotopes
503 in tree rings: towards a mechanistic understanding of isotope fractionation and mixing processes
504 from the leaves to the wood, *Tree Physiol.*, 34, 796–818, 2014.

505 Gessler, A., Rennenberg, H., and Keitel, C.: Stable isotope composition of organic compounds
506 transported in the phloem of European beech-evaluation of different methods of phloem sap
507 collection and assessment of gradients in carbon isotope composition during leaf-to-stem transport,
508 *Plant Biology*, 6, 721–729, 2004.

509 Gessler, A., Tcherkez, G., Peuke, A. D., Ghashghaie, J., and Farquhar, G. D.: Experimental evidence
510 for diel variations of the carbon isotope composition in leaf, stem and phloem sap organic matter
511 in *Ricinus communis*, *Plant Cell Environ.*, 31, 941–953, 2008.

512 Gillon, J. S., Griffiths, H.: The influence of (photo)respiration on carbon isotope discrimination in
513 plants. *Plant Cell Environ.*, 20, 1217–1230, 1997.

514 Gleixner, G. and Schmidt, H.: Carbon isotope effects on the fructose-1, 6-bisphosphate aldolase
515 reaction, origin for non-statistical ¹³C distributions in carbohydrates, *J. Biol. Chem.*, 272, 5382–
516 5387, 1997.

517 Guy, R. D., Fogel, M. L., and Berry, J. A.: Photosynthetic fractionation of the stable isotopes of oxygen
518 and carbon, *Plant Physiol.*, 101, 37–47, 1993.

519 Han, J. M., Meng, H. F., Wang, S. Y., Jiang, C. D., Liu, F., Zhang, W. F., and Zhang, Y. L.: Variability
520 of mesophyll conductance and its relationship with water use efficiency in cotton leaves under
521 drought pretreatment, *J. Plant Physiol.*, 194, 61–71, 2016.

522 Hommel, R., Siegwolf, R., Saurer, M., Farquhar, G. D., Kayler, Z., Ferrio, J. P., and Gessler, A.:
523 Drought response of mesophyll conductance in forest understory species-impacts on water-use
524 efficiency and interactions with leaf water movement, *Physiol. Plantarum*, 152, 98–114, 2014.

525 Igamberdiev, A. U., Mikkelsen, T. N., Ambus, P., Bauwe, H., and Lea, P. J.: Photorespiration
526 contributes to stomatal regulation and carbon isotope fractionation: a study with barley, potato and
527 *Arabidopsis* plants deficient in glycine decarboxylase, *Photosynth. Res.*, 81, 139–152, 2004.

528 IPCC: Summary for policymakers, in: *Climate Change 2014, Mitigation of Climate Change*,

529 contribution of Working Group III to the Fifth Assessment Report of the Intergovernmental Panel
530 on Climate Change, edited by: Edenhofer, O., Pichs-Madruga, R., Sokona, Y., Farahani, E.,
531 Kadner, S., Seyboth, K., Adler, A., Baum, I., Brunner, S., Eickemeier, P., Kriemann, B.,
532 Savolainen, J., Schlomer, S., von Stechow, C., Zwickel, T., and Minx, J. C., Cambridge
533 University Press, Cambridge, UK and New York, NY, USA, 1–30, 2014.

534 Jäggi, M., Saurer, M., Fuhrer, J., and Siegwolf, R.: The relationship between the stable carbon isotope
535 composition of needle bulk material, starch, and tree rings in *Picea abies*, *Oecologia*, 131, 325–
536 332, 2002.

537 Kadam, N. N., Xiao, G., Melgar, R. J., Bahuguna, R. N., Quinones, C., Tamilselvan, A., Prasad, P. V.
538 V., and Jagadish, K. S. V.: Chapter three-agronomic and physiological responses to high
539 temperature, drought, and elevated CO₂ interactions in cereals, *Adv. Agron.*, 127, 111–156, 2014.

540 Kgope, B. S., Bond, W. J., and Midgley, G. F.: Growth responses of African savanna trees implicate
541 atmospheric [CO₂] as a driver of past and current changes in savanna tree cover, *Austral Ecol.*, 35,
542 451–463, 2010.

543 Kirkham, M. B.: Elevated carbon dioxide: impacts on soil and plant water relations, CRC Press,
544 London, New York, 2016.

545 Kodama, N., Barnard, R. L., Salmon, Y., Weston, C., Ferrio, J. P., Holst, J., Werner, R. A., Saurer, M.,
546 Rennenberg, H., and Buchmann, N.: Temporal dynamics of the carbon isotope composition in a
547 *Pinus sylvestris* stand: from newly assimilated organic carbon to respired carbon dioxide,
548 *Oecologia*, 156, 737–750, 2008.

549 Lanigan, G. J., Betson, N., Griffiths, H., and Seibt, U.: Carbon isotope fractionation during
550 photorespiration and carboxylation in *Senecio*, *Plant Physiol.*, 148, 2013–2020, 2008.

551 Le Roux, X., Bariac, T., Sinoquet H., Genty, B., Piel, C., Mariotti, A., Girardin, C., and Richard, P.:
552 Spatial distribution of leaf water-use efficiency and carbon isotope discrimination within an
553 isolated tree crown, *Plant Cell Environ.*, 24, 1021–1032, 2001.

554 Leakey, A. D.: Rising atmospheric carbon dioxide concentration and the future of C4 crops for food
555 and fuel, *Proceedings of the Royal Society of London B: Biological Sciences*, 276, 1517–2008,
556 2009.

557 Leakey, A. D., Ainsworth, E. A., Bernacchi, C. J., Rogers, A., Long, S. P., and Ort, D. R.: Elevated
558 CO₂ effects on plant carbon, nitrogen, and water relations: six important lessons from FACE, *J.*
559 *Exp. Bot.*, 60, 2859–2876, 2009.

560 Lobell, D. B., Roberts, M. J., Schlenker, W., Braun, N., Little, B. B., Rejesus, R. M., and Hammer, G.
561 L.: Greater sensitivity to drought accompanies maize yield increase in the US Midwest, *Science*,
562 344, 516–519, 2014.

563 Medlyn, B. E., Barton, C. V. M., Broadmeadow, M. S. J., Ceulemans, R., Angelis, P. D., Forstreuter,
564 M., Freeman, M., Jackson, S. B., Kellomäki, S., and Laitat, E.: Stomatal conductance of forest
565 species after long-term exposure to elevated CO₂ concentration: a synthesis, *New Phytol.*, 149,
566 247–264, 2001.

567 Mielke, M. S., Oliva, M. A., de Barros, N. F., Penchel, R. M., Martinez, C. A., Da Fonseca, S., and de
568 Almeida, A. C.: Leaf gas exchange in a clonal eucalypt plantation as related to soil moisture, leaf
569 water potential and microclimate variables, *Trees*, 14, 263–270, 2000.

570 Miranda Apodaca, J., Pérez López, U., Lacuesta, M., Mena Petite, A., and Muñoz Rueda, A.: The type
571 of competition modulates the ecophysiological response of grassland species to elevated CO₂ and
572 drought, *Plant Biolog*, 17, 298–310, 2015.

573 Parker, W. C. and Pallardy, S. G.: Gas exchange during a soil drying cycle in seedlings of four black
574 walnut (*Juglans nigra* L.) Families, *Tree physiol.*, 9, 339–348, 1991.

575 Pons, T. L., Flexas, J., von Caemmerer, S., Evans, J. R., Genty, B., Ribas-Carbo, M., and Brugnoli, E.:
576 Estimating mesophyll conductance to CO₂: methodology, potential errors, and recommendations,
577 *J. Exp. Bot.*, 8, 1–18, 2009.

578 Reich, P. B., Walters, M. B., and Tabone, T. J.: Response of *Ulmus americana* seedlings to varying
579 nitrogen and water status. 2 Water and nitrogen use efficiency in photosynthesis, *Tree Physiol.*, 5,
580 173–184, 1989.

581 Rinne, K. T., Saurer, M., Kirdeyanov, A. V., Bryukhanova, M. V., Prokushkin, A. S., Churakova
582 Sidorova, O. V., and Siegwolf, R. T.: Examining the response of larch needle carbohydrates to
583 climate using compound-specific δ¹³C and concentration analyses, EGU General Assembly
584 Conference, 1814949R, 2016.

585 Robredo, A., Pérez-López, U., de la Maza, H. S., González-Moro, B., Lacuesta, M., Mena-Petite, A.,
586 and Muñoz-Rueda, A.: Elevated CO₂ alleviates the impact of drought on barley improving water
587 status by lowering stomatal conductance and delaying its effects on photosynthesis, *Environ. Exp.*
588 *Bot.*, 59, 252–263, 2007.

589 Robredo, A., Pérez-López, U., Lacuesta, M., Mena-Petite, A., and Muñoz-Rueda, A.: Influence of
590 water stress on photosynthetic characteristics in barley plants under ambient and elevated CO₂
591 concentrations, *Biologia. Plantarum*, 54, 285–292, 2010.

592 Rossmann, A., Butzenlechner, M., and Schmidt, H.: Evidence for a nonstatistical carbon isotope
593 distribution in natural glucose, *Plant Physiol.*, 96, 609–614, 1991.

594 Streit, K., Rinne, K. T., Hagedorn, F., Dawes, M. A., Saurer, M., Hoch, G., Werner, R. A., Buchmann,
595 N., and Siegwolf, R. T. W.: Tracing fresh assimilates through *Larix decidua* exposed to elevated
596 CO₂ and soil warming at the alpine treeline using compound-specific stable isotope analysis, *New*
597 *Phytol.*, 197, 838–849, 2013.

598 Tausz Posch, S., Norton, R. M., Seneweera, S., Fitzgerald, G. J., and Tausz, M.: Will intra-specific
599 differences in transpiration efficiency in wheat be maintained in a high CO₂ world? A FACE study,
600 *Physiol. Plantarum*, 148, 232–245, 2013.

601 Tazoe, Y., von Caemmerer, S., Estavillo, G. M., and Evans, J. R.: Using tunable diode laser
602 spectroscopy to measure carbon isotope discrimination and mesophyll conductance to CO₂
603 diffusion dynamically at different CO₂ concentrations, *Plant Cell Environ.*, 34, 580–591, 2011.

604 Terashima, I., Hanba, Y.T., Tazoe, Y., Vyas, P., and Yano, S.: Irradiance and phenotype: comparative
605 eco-development of sun and shade leaves in relation to photosynthetic CO₂ diffusion, *J. Exp. Bot.*,
606 57, 343–354, 2006.

607 Théroux-Rancourt, G., Éthier, G., and Pepin, S.: Threshold response of mesophyll CO₂ conductance to
608 leaf hydraulics in highly transpiring hybrid poplar clones exposed to soil drying, *J. Exp. Bot.*, 65,
609 741–753, 2014.

610 Von Caemmerer, S. V. and Farquhar, G. D.: Some relationships between the biochemistry of
611 photosynthesis and the gas exchange of leaves, *Planta*, 153, 376–387, 1981.

612 Wall, G. W., Garcia, R. L., Kimball, B. A., Hunsaker, D. J., Pinter, P. J., Long, S. P., Osborne, C. P.,
613 Hendrix, D. L., Wechsung, F., and Wechsung, G.: Interactive effects of elevated carbon dioxide
614 and drought on wheat, *Agron. J.*, 98, 354–381, 2006.

615 Wall, G. W., Garcia, R. L., Wechsung, F., and Kimball, B. A.: Elevated atmospheric CO₂ and drought
616 effects on leaf gas exchange properties of barley, *Agr. Ecosyst. Environ.*, 144, 390–404, 2011.

617 Warren, C. R. and Adams, M. A.: Internal conductance does not scale with photosynthetic capacity:
618 implications for carbon isotope discrimination and the economics of water and nitrogen use in
619 photosynthesis, *Plant Cell Environ.*, 29, 192–201, 2006.
620 Xu, D. Q.: Some problems in stomatal limitation analysis of photosynthesis, *Plant Physiol. J.*, 33, 241–
621 244, 1997.
622 Xu, Z. and Zhou, G.: Responses of photosynthetic capacity to soil moisture gradient in perennial
623 rhizome grass and perennial bunchgrass, *BMC Plant Boil.*, 11, 21, 2011.
624 Yang, B., Pallardy, S. G., Meyers, T. P., GU, L. H., Hanson, P. J., Wullschleger, S. D., Heuer, M.,
625 Hosman, K. P., Riggs, J. S., and Sluss D. W.: Environmental controls on water use efficiency
626 during severe drought in an Ozark Forest in Missouri, USA, *Global Change Biol.*, 16, 2252–2271,
627 2010.
628 Yu, G., Wang, Q., and Mi, N.: *Ecophysiology of plant photosynthesis, transpiration, and water use*,
629 Science Press, Beijing, China, 2010.

630

631 **Author contributions**

632 N. Zhao and Y. He collected field samples, and performed experiments. N. Zhao performed data
633 analysis and wrote the paper. P. Meng commented on the theory and study design. X. Yu revised and
634 edited the manuscript.

635

636 *Acknowledgements.* Financial support for this project was provided by the National Natural Science
637 Foundation of China (grant No. 41430747) and the Beijing Municipal Education Commission
638 (CEFF-PXM2017_014207_000043). We thank Beibei Zhou and Yuanhai Lou for collection of
639 materials and management of saplings. We are grateful to anonymous reviewers for constructive
640 suggestions regarding this manuscript. Due to space limitations we cited selected references involving
641 this study topic and apologize for authors whose work was not cited.

642

643

644

645

646

647

648

649

650

651

652

653

654

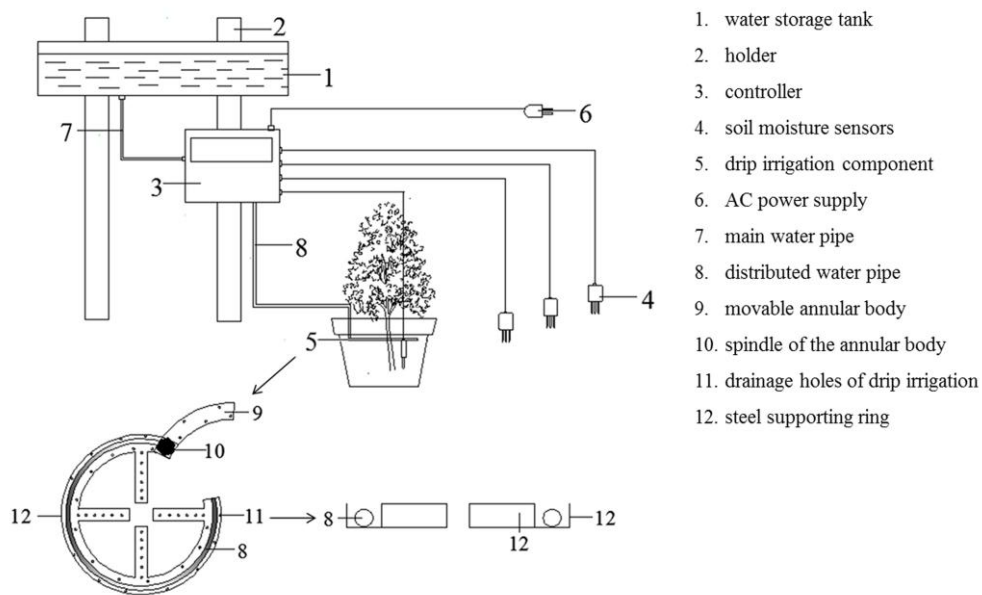
655

656

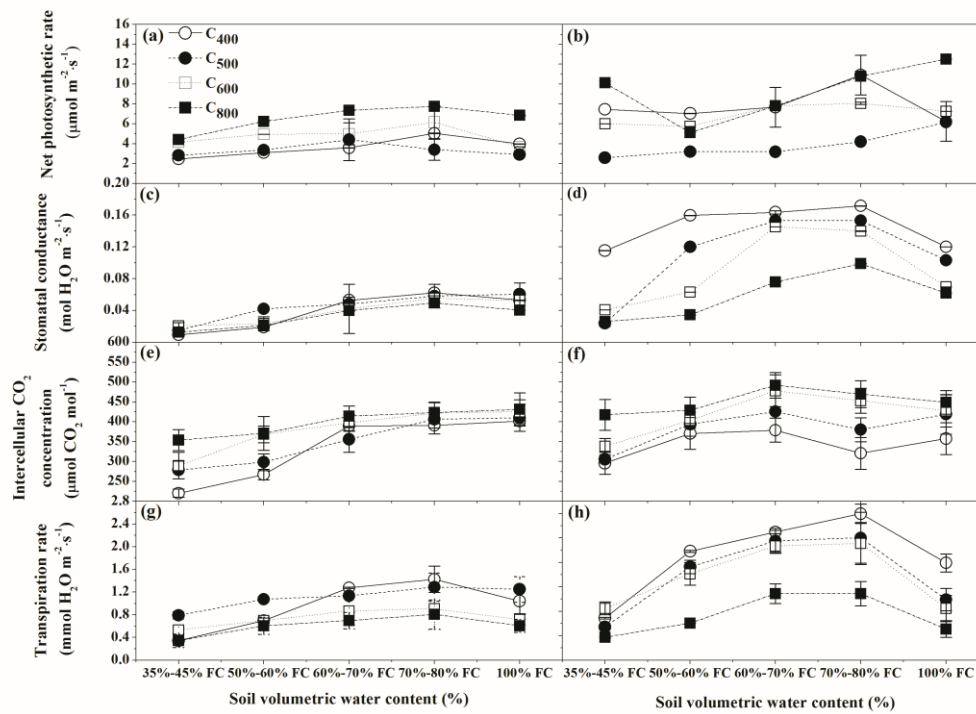
657

658

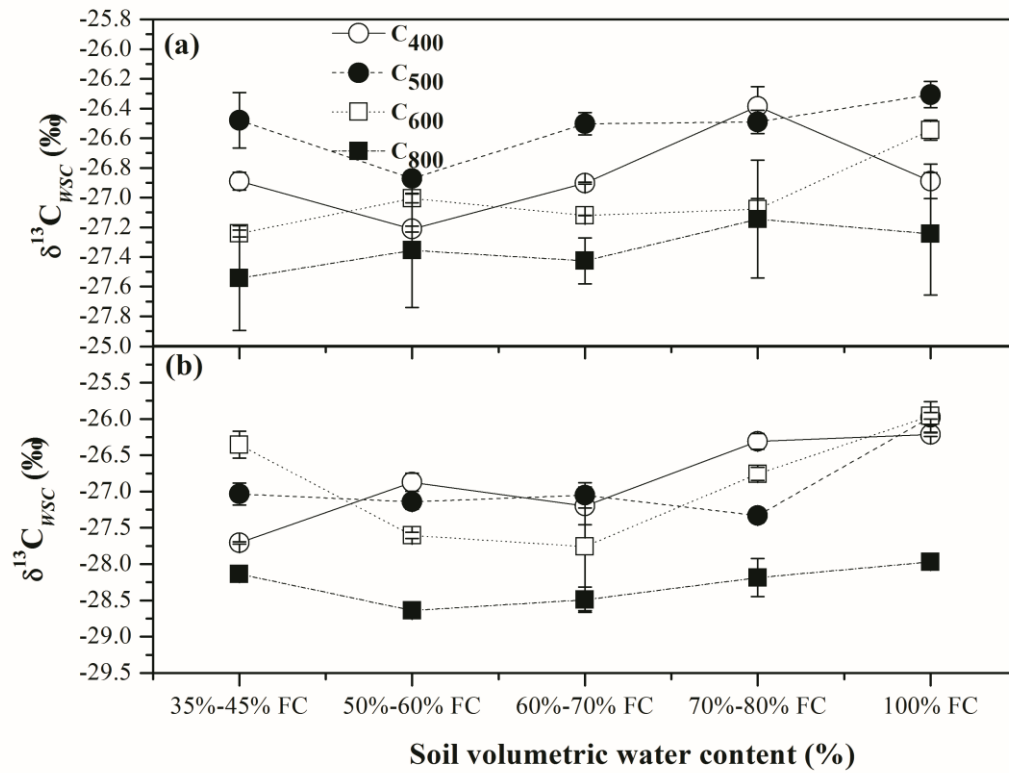
659



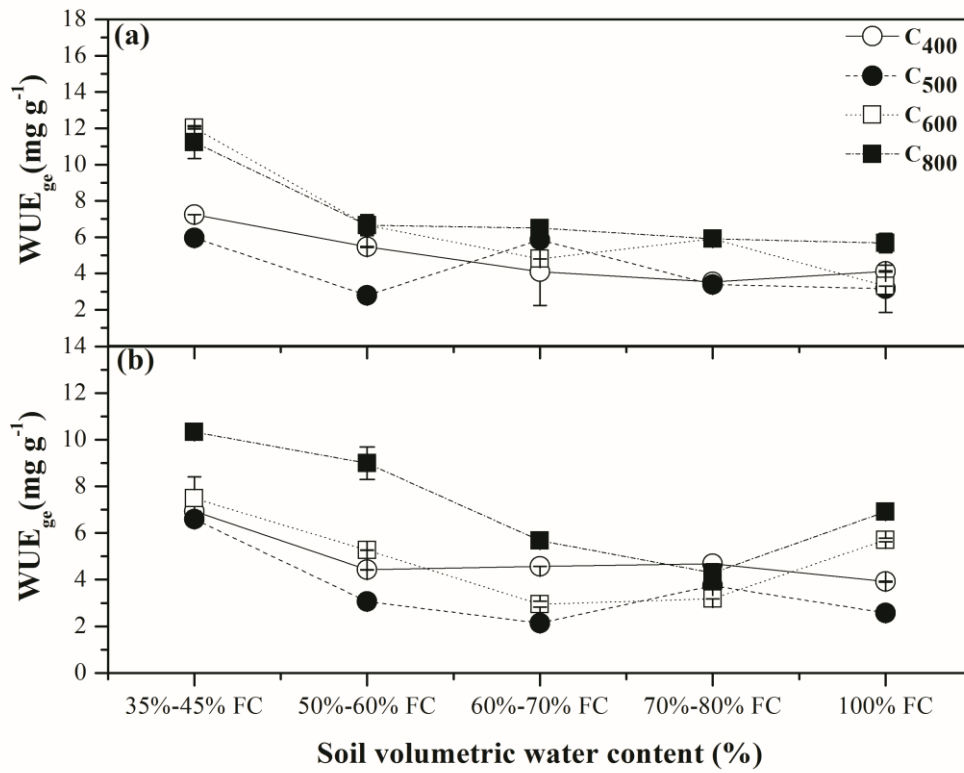
661 **Figure 1.** Diagram of the automatic drip irrigation device **used in this study**; **numbers** indicate the
 662 individual parts of **the irrigation** device (No. 1–12). The lower-left corner of this figure presents the
 663 detailed schematic for the drip irrigation **component** (No. 8–12).



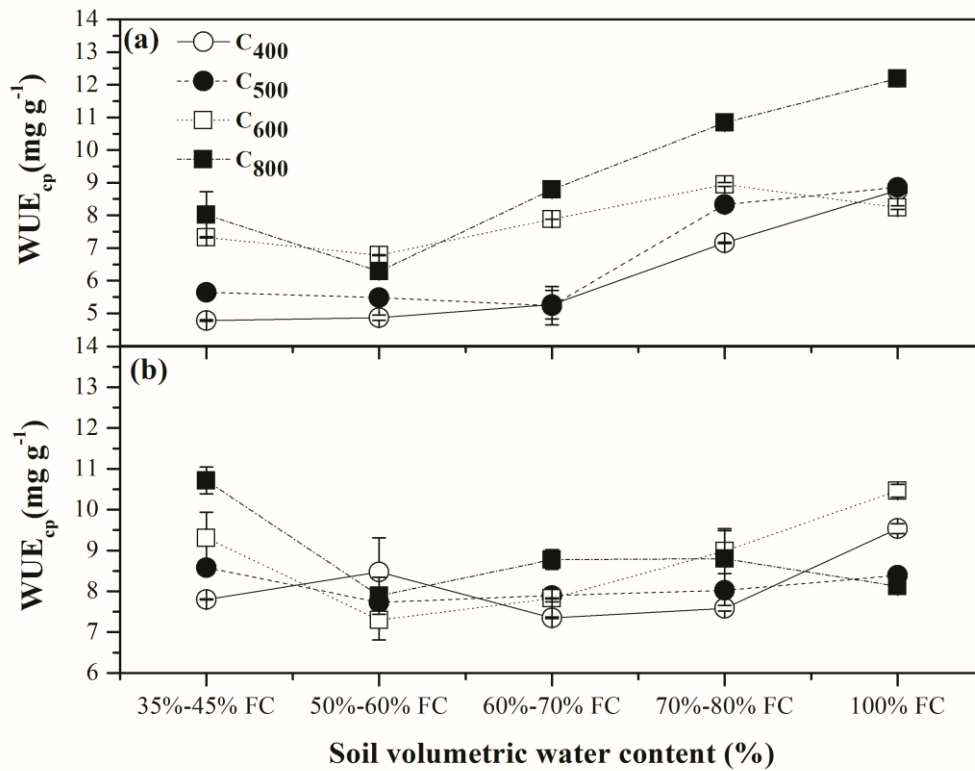
664 **Figure 2.** Net photosynthetic rates (P_n , $\mu\text{mol m}^{-2} \text{s}^{-1}$, a and b), stomatal conductance (g_s , $\text{mol H}_2\text{O m}^{-2}$
665 s^{-1} , c and d), intercellular CO_2 concentration (C_i , $\mu\text{mol CO}_2 \text{mol}^{-1}$, e and f), and transpiration rates (T_r ,
666 $\text{mmol H}_2\text{O m}^{-2} \text{s}^{-1}$, g and h) in *P. orientalis* and *Q. variabilis* for four CO_2 concentrations \times five soil
667 volumetric water content treatments. Means \pm SDs, $n=32$.



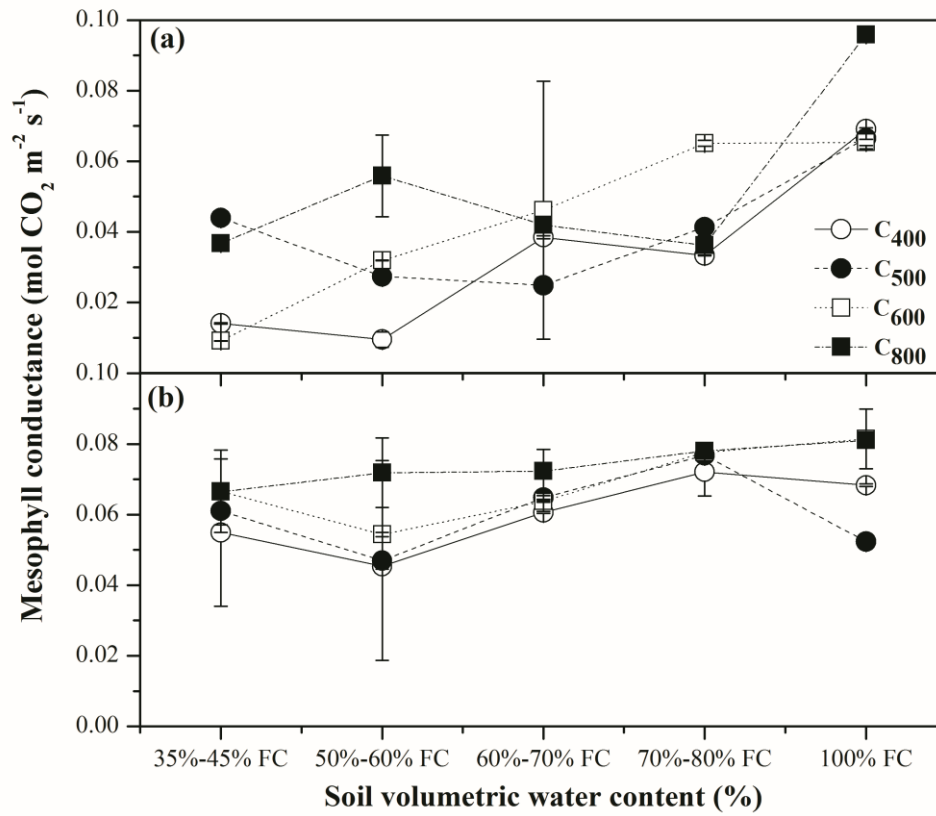
668 **Figure 3.** Carbon isotope composition of water-soluble compounds ($\delta^{13}C_{WSC}$) extracted from leaves of
 669 *P. orientalis* (a) and *Q. variabilis* (b) for four CO₂ concentrations \times five soil volumetric water content
 670 treatments. Means \pm SDs, n= 32.



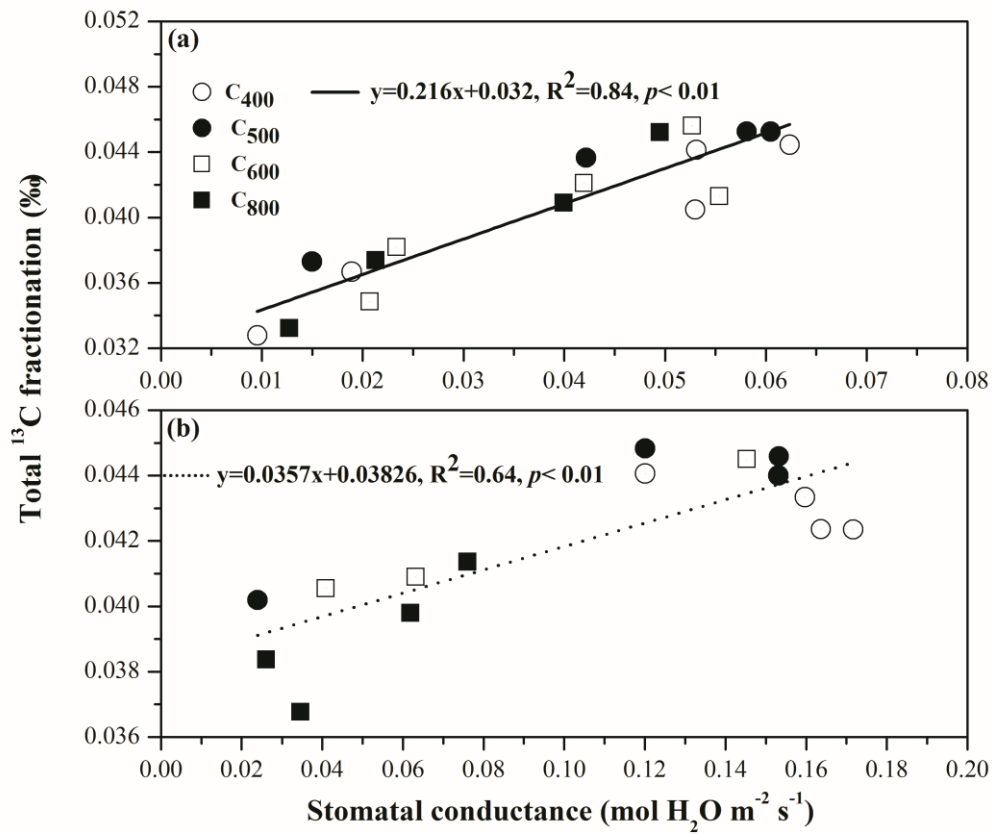
671 **Figure 4.** Instantaneous water use efficiency through gas exchange measurements (WUE_{ge}) for leaves
 672 from *P. orientalis* (a) and *Q. variabilis* (b) for four CO₂ concentrations × five soil volumetric water
 673 content treatments. Means ±SDs, n= 32.



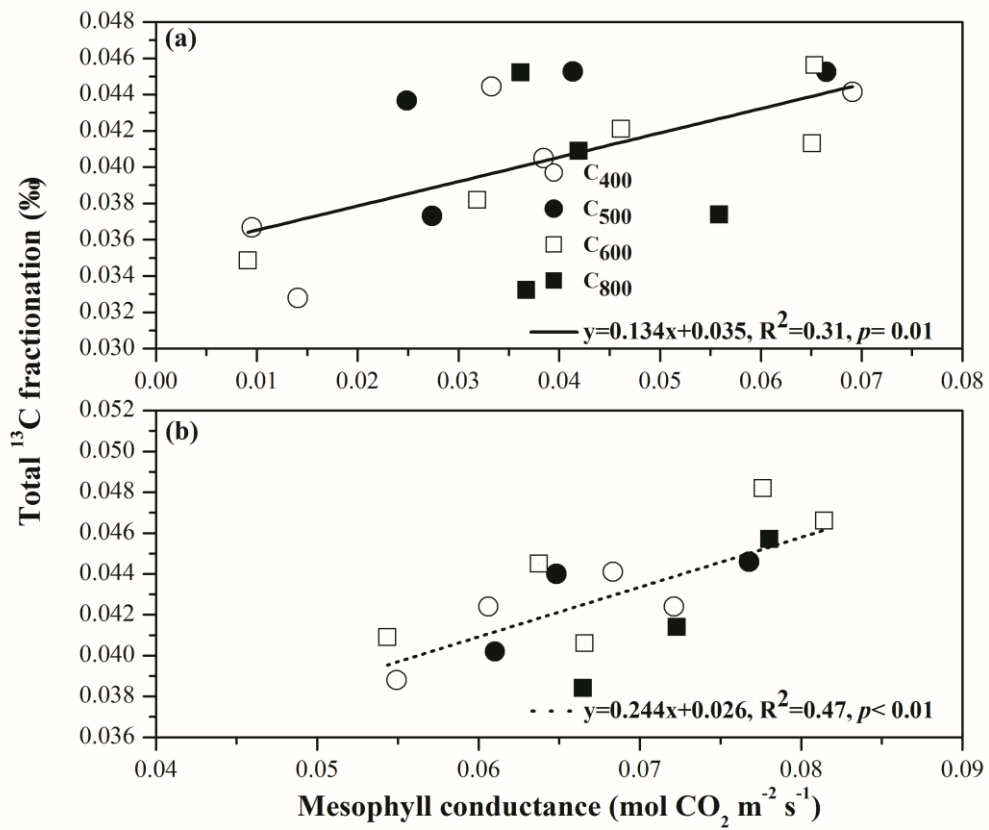
674 **Figure 5.** Instantaneous water use efficiency estimated by $\delta^{13}\text{C}$ of water-soluble compounds (WUE_{cp})
 675 from leaves of *P. orientalis* (a) and *Q. variabilis* (b) for four CO_2 concentrations \times five soil volumetric
 676 water content treatments. Means \pm SDs, $n=32$.



677 **Figure 6.** Mesophyll conductance in *P. orientalis* (a) and *Q. variabilis* (b) for four CO₂ concentrations
 678 × five soil volumetric water content treatments. Means ±SDs, n= 32.



679 **Figure 7.** Regression between stomatal conductance and total ^{13}C fractionation in *P. orientalis* (a) and
 680 *Q. variabilis* (b) for four CO_2 concentrations \times five soil volumetric water content treatments ($p = 0.01$,
 681 $n = 32$).



682 **Figure 8.** Regression between mesophyll conductance and total ^{13}C fractionation in *P. orientalis* (a)
 683 and *Q. variabilis* (b) for four CO₂ concentrations \times five soil volumetric water content treatments ($p=$
 684 0.01, $n=32$).

Table

Table 1. Orthogonal treatments applied to *P. orientalis* and *Q. variabilis*.

<i>P. orientalis</i>	Repeats (cultivated period)	B ₁	B ₂	B ₃	B ₄	B ₅
A ₁	R ₁ :June 2–9	A ₁ B ₁ R ₁	A ₁ B ₂ R ₁	A ₁ B ₃ R ₁	A ₁ B ₄ R ₁	A ₁ B ₅ R ₁
	R ₂ :June 12–19	A ₁ B ₁ R ₂	A ₁ B ₂ R ₂	A ₁ B ₃ R ₂	A ₁ B ₄ R ₂	A ₁ B ₅ R ₂
A ₂	R ₁ :July 11–18	A ₂ B ₁ R ₁	A ₂ B ₂ R ₁	A ₂ B ₃ R ₁	A ₂ B ₄ R ₁	A ₂ B ₅ R ₁
	R ₂ :July 22–29	A ₂ B ₁ R ₂	A ₂ B ₂ R ₂	A ₂ B ₃ R ₂	A ₂ B ₄ R ₂	A ₂ B ₅ R ₂
A ₃	R ₁ :June 2–9	A ₃ B ₁ R ₁	A ₃ B ₂ R ₁	A ₃ B ₃ R ₁	A ₃ B ₄ R ₁	A ₃ B ₅ R ₁
	R ₂ :June 12–19	A ₃ B ₁ R ₂	A ₃ B ₂ R ₂	A ₃ B ₃ R ₂	A ₃ B ₄ R ₂	A ₃ B ₅ R ₂
A ₄	R ₁ :July 11–18	A ₄ B ₁ R ₁	A ₄ B ₂ R ₁	A ₄ B ₃ R ₁	A ₄ B ₄ R ₁	A ₄ B ₅ R ₁
	R ₂ :July 22–29	A ₄ B ₁ R ₂	A ₄ B ₂ R ₂	A ₄ B ₃ R ₂	A ₄ B ₄ R ₂	A ₄ B ₅ R ₂
<i>Q. variabilis</i>	Repeats (cultivated period)	B ₁	B ₂	B ₃	B ₄	B ₅
A ₁	P ₁ :June 21–28	A ₁ B ₁ P ₁	A ₁ B ₂ P ₁	A ₁ B ₃ P ₁	A ₁ B ₄ P ₁	A ₁ B ₅ P ₁
	P ₂ :July 2–9	A ₁ B ₁ P ₂	A ₁ B ₂ P ₂	A ₁ B ₃ P ₂	A ₁ B ₄ P ₂	A ₁ B ₅ P ₂
A ₂	P ₁ :August 4–11	A ₂ B ₁ P ₁	A ₂ B ₂ P ₁	A ₂ B ₃ P ₁	A ₂ B ₄ P ₁	A ₂ B ₅ P ₁
	P ₂ :August 15–22	A ₂ B ₁ P ₂	A ₂ B ₂ P ₂	A ₂ B ₃ P ₂	A ₂ B ₄ P ₂	A ₂ B ₅ P ₂
A ₃	P ₁ :June 21–28	A ₃ B ₁ P ₁	A ₃ B ₂ P ₁	A ₃ B ₃ P ₁	A ₃ B ₄ P ₁	A ₃ B ₅ P ₁
	P ₂ :July 2–9	A ₃ B ₁ P ₂	A ₃ B ₂ P ₂	A ₃ B ₃ P ₂	A ₃ B ₄ P ₂	A ₃ B ₅ P ₂
A ₄	P ₁ :August 4–11	A ₄ B ₁ P ₁	A ₄ B ₂ P ₁	A ₄ B ₃ P ₁	A ₄ B ₄ P ₁	A ₄ B ₅ P ₁
	P ₂ :August 15–22	A ₄ B ₁ P ₂	A ₄ B ₂ P ₂	A ₄ B ₃ P ₂	A ₄ B ₄ P ₂	A ₄ B ₅ P ₂

Table 2. Carbon-13 isotope fractionation in *P. orientalis* and *Q. variabilis* under four CO₂ concentrations × five soil volumetric water content treatments.

Species	SWC (of FC)	CO ₂ concentration (ppm)													
		¹³ C				¹³ C									
		400	500	600	800	fractionation (‰)	400	500	600	800	fractionation (‰)	400	500	600	800
<i>P. orientalis</i>	35%–45%	0.0328	0.0373	0.0349	0.0332		0.0081	0.0030	0.0034	0.0072		0.0247	0.0343	0.0315	0.0260
	50%–60%	0.0367	0.0437	0.0382	0.0374		0.0018	0.0058	0.0094	0.0004		0.0349	0.0379	0.0288	0.0370
	60%–70%	0.0405	0.0366	0.0421	0.0409		0.0018	0.0050	0.0026	0.0007		0.0387	0.0316	0.0395	0.0402
	70%–80%	0.0444	0.0453	0.0413	0.0452		0.0044	0.0052	0.0103	0.0013		0.0400	0.0401	0.0310	0.0439
	100%	Total ¹³ C fractionatio n (‰)	0.0441	0.0453	0.0456	0.0472	Mesophyll conductance	0.0057	0.0040	0.0025	0.0039	Post- photosynthesis	0.0384	0.0413	0.0431
<i>Q. variabilis</i>	35%–45%	0.0388	0.0402	0.0406	0.0384		0.0007	0.0025	0.0006	0.0091		0.0381	0.0377	0.0400	0.0293
	50%–60%	0.0433	0.0448	0.0409	0.0368		0.0061	0.0084	0.0023	0.0018		0.0372	0.0364	0.0386	0.0350
	60%–70%	0.0424	0.0440	0.0445	0.0414		0.0066	0.0086	0.0078	0.0041		0.0358	0.0354	0.0367	0.0373
	70%–80%	0.0424	0.0446	0.0482	0.0457		0.0034	0.0016	0.0074	0.0028		0.0390	0.0430	0.0408	0.0429
	100%		0.0441	0.0466	0.0466	0.0398		0.0027	0.0076	0.0022	0.0125		0.0414	0.0390	0.0444